Bulletin of the Seismological Society of America, Vol. 95, No. 3, pp. 1202–1208, June 2005, doi: 10.1785/0120040098

Broadband Seismic Noise Analysis of the Himalayan Nepal Tibet Seismic Experiment

by Thomas L. de la Torre and Anne F. Sheehan

Abstract We analyze background noise to assess the effects of experimental temporary seismic vault construction and to determine the time needed for noise at sites to stabilize after deployment noise as part of the Himalayan Nepal Tibet Seismic Experiment (HIMNT). We calculated power spectral densities of background noise for each component of each broadband seismometer deployed in Nepal and Tibet and then compared them with the high-noise model and low-noise Model of Peterson (1993). All segments from day and night local time windows were included in the calculation without parsing out earthquakes. Noise levels were considerably higher for the Nepal stations than the Tibet stations, in particular, in the high frequencies. The most northern of the stations in Tibet show unexpected day/night differences of ~10–20 dB for the vertical components, which is significantly greater than the day/night differences of the horizontal components. However, all the stations show noise levels concordant with microseism peak levels. Power spectral density estimates show moderate noise levels with all stations falling within the high and low bounds of Peterson (1993), except for the southern Nepal stations, which were built above ground and exceed the high-noise model at frequencies >1.0 Hz. The time needed for noise at a site to stabilize was ~1–5 days after deployment.

Introduction

The Himalayan Nepal Tibet Seismic Experiment (HIMNT), a joint Program for Array Seismic Studies of Continental Lithosphere (PASSCAL) broadband seismic project of the University of Colorado at Boulder, State University of New York–Binghamton, the Department of Mines and Geology of Nepal, and the Institute of Geology and Geophysics of the Chinese Academy of Science, examines the Himalayan Mountain building processes through earthquake location, crust and mantle imaging, and geometric analysis of subsurface folds and thrust faults. Noise from natural and anthropogenic sources in a seismic signal hinders the ability to extract details required for such an analysis. The less noise at a station, the more earthquakes the station can detect. We conducted an analysis of noise to quantify and characterize the seismic noise levels at sites in this experiment to help identify site conditions for future experiments similar to HIMNT.

Twenty-eight broadband seismometers were deployed from the fall 2001 to fall 2002 in populated and remote sites in eastern Nepal and southern Tibet (Fig. 1). Each site contained a Streckeisen STS2 broadband seismometer with Reftek data-acquisition systems continually sampling at 1 and 40 samples per second. Some of these sensors were housed in experimentally designed vaults and most of these sensor locations had not been previously utilized for a broadband experiment. A primary concern was the performance of stations at these sites. In particular, two sensors were located on the Terai-Ganges River Plain housed in two different above-ground vault types, and elsewhere sensors were coupled with and without cement to plastic containers. We posed the following questions: How did the noise levels in the HIMNT compare with the U.S. Geological Survey (USGS) noise model? How much noisier was one vault type than other types? How much time passed before a station stabilized or maintained constant noise levels?

We divide the noise spectrum into three frequency bands: long period, 0.01–0.1 Hz; "microseism," 0.1–1.0 Hz; and short period, 1.0–10 Hz. Tilt, pressure, and wind are the sources of noise at long periods that can quickly raise the noise of the horizontal components in broadband data. Ocean waves create the microseism noise that peak at 0.2 Hz with a secondary peak between 0.05 and 0.1 Hz. For continental sites, cultural noise and local weather conditions dictate the noise at frequencies >1.0 Hz (Peterson, 1993; Webb, 1998).

The Power Spectral Density Calculation

We calculated power spectral densities (PSDs) of noise for each component at each station by extracting 3-h seg-

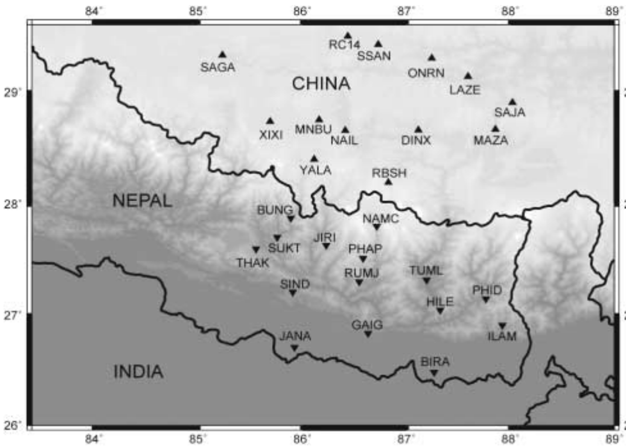

Figure 1. HIMNT station map. Tibet stations are triangles and Nepal stations are inverted triangles. GSN station LSA, latitude 29.70° N, longitude 91.12° E, is located northeast of the Tibet stations.

ments at night, hours 0200–0500, and day, hours 0900–1200, local time from the HIMNT database without filtering for earthquakes. After deconvolving the instrument response, we estimated power spectra by time averaging over modified periodograms (Welch, 1967) in Matlab by Math Works Inc. Each segment was divided into eight 1350-sec sections with 50% overlap and then Fourier transformed. To properly compare our PSD calculation with the USGS noise models we ran HIMNT data sets through the algorithm Peterson used to calculate the USGS noise models (Peterson, 1993) and compared PSD. We found that the algorithms produced the same PSDs at the same frequencies with slight differences because of different averaging parameters. To represent the stations' typical noise spectra at each frequency, we removed the highest 5% and lowest 5% of the spectral estimates before calculating 95% confidence intervals, $1.96 \times$ standard deviation of the amplitudes over the frequency range (Wilson *et al.*, 2002). We compared the median PSD of HIMNT with the east, north, and vertical components of the Guralp CMG-3T broadband sensor at station LSA, a Global Seismic Network (GSN) station located ~315 km northeast of the Tibet array. The median PSDs for station LSA were calculated from 10-min data windows with 50% overlap for entire days from two weeks in January 2002, from two weeks in July 2002, and from two weeks in October 2002 (H. Bolton, personal comm., 2004).

We present the median PSD for the entire Nepal and Tibet arrays (except for stations BIRA and JANA) and station LSA from 0.01 to 10.0 Hz with 95% confidence interval ranges plotted for the Nepal and Tibet arrays (Fig. 2). The differences between the arrays during the day and night are shown in Figure 3. We then compare the PSD for each vault type in Figure 4 and PSD variation over time in Figure 5.

Results and Discussion

In comparing overall median PSD levels of each component of each array with the USGS high- and low-noise models (Peterson, 1993) and with the GSN station LSA, we did not include the PSD levels of the two stations in the Ganges River Plain, stations BIRA and JANA, because they were the noisiest stations, in particular, at high frequencies. Noise levels at both arrays fell within the bounds of the noise models, with all components at similar PSD levels from 0.5 to 10.0 Hz. At the microseism peak from 0.14 to 0.2 Hz (Webb, 1998), the vertical components were noisier than the horizontal components by ~5 dB, but Peterson's (1993) low-noise model still bounded the minimum in both arrays and station LSA. Below 0.1 Hz, the vertical components diverged to quieter noise levels from the horizontal components and reflected the "notch" at 0.03–0.1 Hz (Webb, 1998). (Fig. 2). All components of station LSA diverged further below both arrays, reflecting the superiority of the permanent station over the temporary one at frequencies <0.05 Hz.

Looking at the confidence intervals for each array, the horizontal and vertical components varied similarly across the frequency range (Fig. 2). At the microseism peak, the PSD levels of both arrays varied by less than ~5 dB. The confidence interval plots showed that the Tibet array noise levels varied more, by ~8–12 dB, than the Nepal array at long periods and at short periods by ~2–6 dB, even though the stations in Tibet were located in more remote sites. The stations in Nepal averaged 314 days of data acquisition so that high and low seasonal noise could have reduced the PSD variation. On the other hand, the stations in Tibet averaged 175 days of data acquisition, including six stations operating from late July to early November 2002. The larger confidence interval range in the Tibet array PSD levels could have been biased toward one period of the year (Fig. 2).

In the microseism range (0.1–1.0 Hz), differences between the arrays decreased to approximately 0 to 5 dB with a small difference plateau of ~1 dB at 0.2 Hz. This small difference shows the dominance of the microseism peak in both regions. The 0 to 5 dB could be explained by a tapering off of the microseisms moving further away from the oceans, because the Tibet array was more continentally isolated than the Nepal stations. At long periods (<0.1 Hz), noise on the horizontal components of the Tibet stations was greater than that in Nepal during the night (0–5 dB) but during the day the horizontal components were quieter by ~0–3 dB. We considered these long-period differences to be insignificant because the confidence bounds of the Tibet array were greater than the bounds of Nepal by 8–12 dB.

Day and Night Comparisons

One can distinguish cultural noise from natural noise by observing day and night patterns (Peterson, 1993). We calculated the day/night variations of each array by subtracting

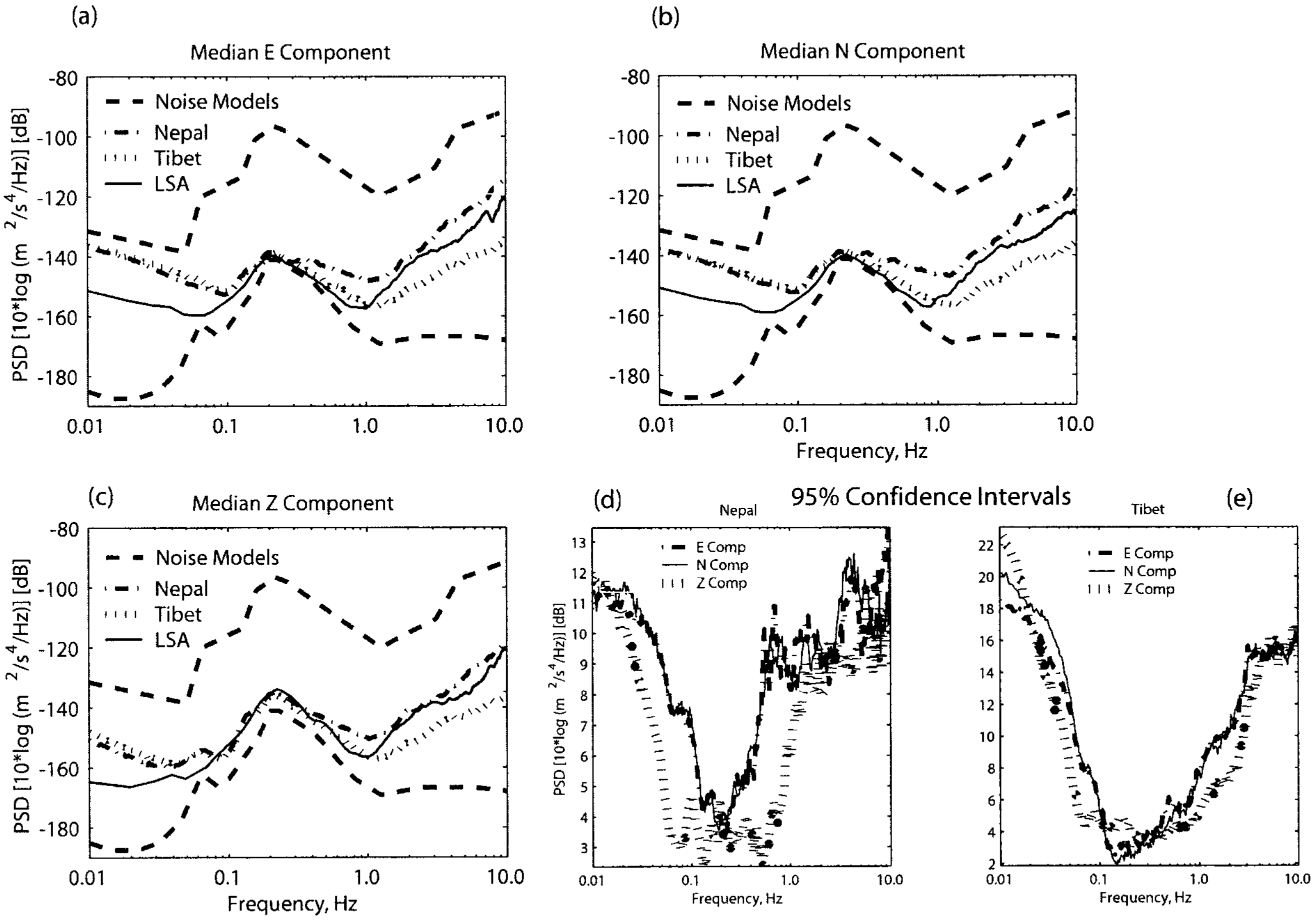

Figure 2. Median PSD of Nepal and Tibet arrays. (a) E component, (b) N component, and (c) Z component. The north and vertical component median PSD for station LSA were also plotted on a, b, and c. (d and e) 95% confidence intervals for PSD of each array.

the median PSD of the night from the median PSD of the day for each component of each station and then plotted the median of the differences for each array for each component. Differences of as much as 18 dB at frequencies >1.0 Hz illustrate the influence of cultural noise in both arrays during the day, and the vanishing of differences at 0.14–1.0 Hz shows the dominance of microseisms. All components followed each other in this trend but then diverged at <0.14 Hz (Fig. 3).

The long-period noise sources from tilt, temperature, and pressure made the day/night differences of the horizontal components ~4 dB noisier than the vertical components of the Nepal array. However, we did not observe strong day/night variations for the horizontal components in the Tibet array. The horizontal components overall were noisier than the vertical component by ~10 dB (Fig. 2) but showed small day/night differences (Fig. 3b). The vertical components showed greater day/night variation than the horizontal components by as much as ~7 dB at 0.01–0.05 Hz. In the most northern stations in the Tibet array, the PSD day/night differences for the vertical components fluctuated up to ~20 dB (stations LAZE and MAZA), ~10 dB (stations XIXI, ONRN, and RC14), and ~7 dB (station SSAN), whereas the horizontal PSD levels had slight differences around ~3 dB. Station SAJA, which lies near these stations, did not exhibit the same trends, but showed small vertical noise differences and ~8-dB horizontal noise differences. There must have been a long-period vertical noise source during the day that affected these stations, except station SAJA, and the rest of the Tibet and Nepal array stations (Fig. 1).

Vault Comparisons

A primary goal of this study was to examine the noise levels of different vault constructions used to temporarily house seismic sensors in the ground. For the HIMNT experiment, five distinctly different vault designs were used. For all the stations, a hole was dug into the ground to a depth of ~1 m or until basement rock was reached. At the 14 stations in Tibet, the sensor was then placed inside a metal can with a sponge cover on a concrete pad cemented to bedrock. For seven stations in Nepal, the sensor was placed on a concrete

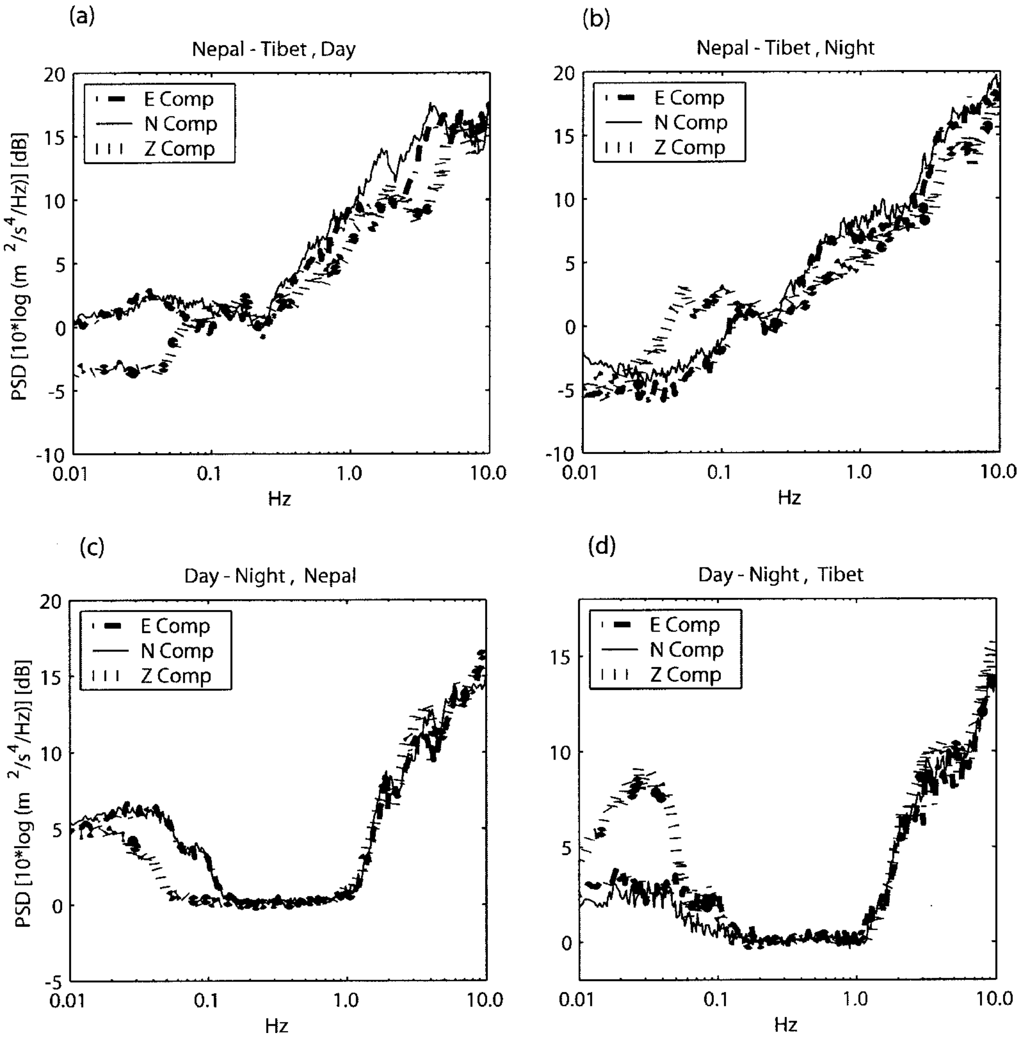

Figure 3. Median of PSD differences between the Nepal array and the Tibet array during the day (a) and night (b) for each component. The median PSD of the Tibet array was subtracted from the median of the Nepal array. Day, 0900–1200 hr local, versus night, 0200–0500 hr local, differences for the Nepal array (c) and Tibet array (d). The median of the night PSDs was subtracted from the median of the day PSDs at each station for each component. Then, the median of the differences for each array was plotted.

pad cemented to soil or bedrock at the base of the hole lined with a plastic cylinder. For five other sites of the Nepal array, concrete was also used to couple the sensor to the plastic bucket. The seismic stations on the Ganges River Plain (JANA and BIRA) were particularly challenging because of the high water table and lack of high ground in the region. Above-ground vaults were constructed at these sites. At station BIRA, a 4 × 4 m wide and 1-m-deep hole was excavated, reinforced with rods, and filled with 20-cm-thick cement. Four cement walls were cast into the hole to a height of 85 cm above ground, filled with rubble and cement core, and then covered with a 10-cm-thick concrete floor. The sensor was placed 20 cm above the ground surface on top of the concrete floor. A downward-inclined pipe leading from the lowest point on the concrete floor permitted cables and water to exit. After a concrete lid was placed over the housing, the whole vault was buried in a mound of mud (Fig. 6a). At station JANA, a hole of width 75 × 75 cm was dug to a depth of 70 cm. A mesh of wire and rebar was inserted into the hole filled with cement with rebar extending vertically out of the hole to ground level. A double wall of bricks 1.3 × 1.3 × 1 m high supported the above-ground portion of the pillar, which was then filled with cement. The sensor was placed in a brick housing constructed on top of the pillar (Fig. 6b).

We compared median PSD levels for five vault types: uncoupled Nepal stations (e.g., TUML), coupled Nepal stations (e.g., BUNG), uncoupled Tibet stations, JANA (concrete pillar), and BIRA (earthen-covered concrete cube) (Fig. 4). The coupled and uncoupled vaults at the stations in

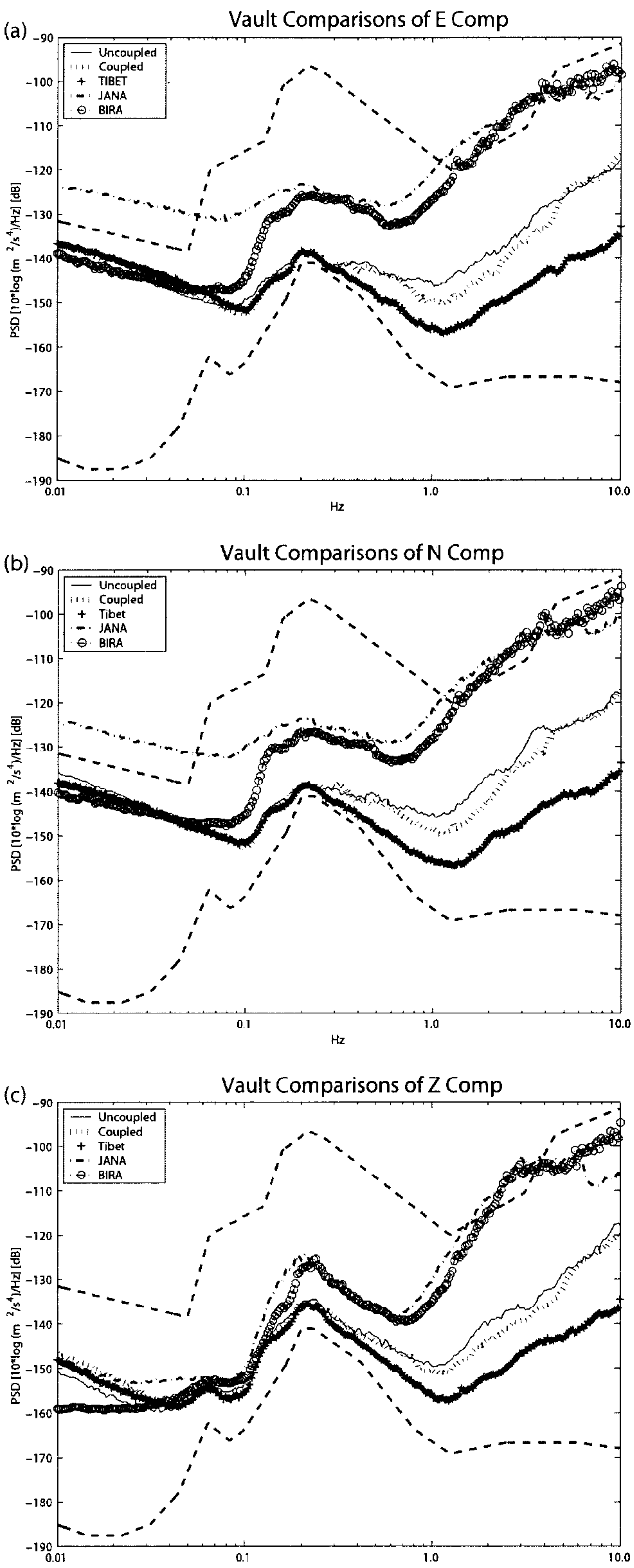

Figure 4. PSD of vault types and associated 95% confidence intervals to the right: (a) east component, (b) north component, and (c) vertical component. Dashed bold lines are the noise-model bounds.

Nepal exhibit nearly equivalent PSD levels above the low-noise model (LNM) through the frequency range ~0.1–10.0 Hz. Microseism sources dominated the noise levels of all the horizontal components (Fig. 4a,b) but the vertical components were noisier by almost ~5 dB (Fig. 4c). At longer periods, the horizontal noise dropped to ~−152 dB at 0.1 Hz, then increased to ~−141 dB through 0.01 Hz. Unlike the horizontal components, the vertical components mirrored the LNM secondary microseism peak at 0.067 Hz, decreasing to ~−160 dB before rising to >−150 dB at 0.01 Hz. The coupled vaults, in general, showed the least amount of variation in all the components, whereas the vertical components of the uncoupled stations varied the most at <0.04 Hz. The uncoupled vaults at the stations in Tibet for all components were the least noisy of all vault types in the high-frequency range ~0.1–10.0 Hz, but mirrored the noise levels of the uncoupled and coupled vaults in Nepal at frequencies <0.1 Hz.

The PSD of the two Ganges River Plain stations, JANA and BIRA, reached levels noisier than the high-noise model (HNM) from 1.0 to 10.0 Hz for all components. However, at the microseism peak, the noise dropped below the HNM but still remained ~15 dB higher than at the other vault constructions. At this frequency, the horizontal components of the two stations diverged. The PSD of the mud-mound station, BIRA, dropped to levels comparable with the coupled and uncoupled vault types whereas the above-ground brick-housing station, JANA, had PSD levels at or above the HNM from <0.06 Hz. This difference in the long periods <0.02 Hz could be caused by the tilting of the brick housing by wind. The vertical components were constantly 10–20 dB higher than the coupled and uncoupled stations in the high-frequency and microseism range but equalized at <0.1 Hz. The quietest station of the two Ganges River Plain stations was BIRA at long periods for all the components and it showed the least noise variation in the vertical components.

Another goal of this study was to examine the time required before noise stabilized after deployment in a temporary vault. Such information is useful in making decisions regarding site stability versus multiple site locations. Night PSDs for the vertical component of each station versus day PSDs after deployment were plotted at periods, 1.0, 20, and 60 sec from 2001 to 2002. PSDs for days that were greater than two standard deviations of the time series were substituted with the time series' mean value to remove high anomalous PSDs. Plots of sample stations housed in each type of vault show immediate leveling off of the PSD for each period (Fig. 5).

For all stations including the stations in Fig. 5, PSD leveled off in 1–5 days. From October 2001 to June 2002, PSD at BUNG (coupled) and at TUML (uncoupled) were at consistent levels on all three period bands. Both stations showed a seasonal rise of ~5–10 dB from June to October 2002 in all the components for 1.0 Hz and increased scatter of PSD at 0.05 and 0.01667 Hz. This scatter at long periods

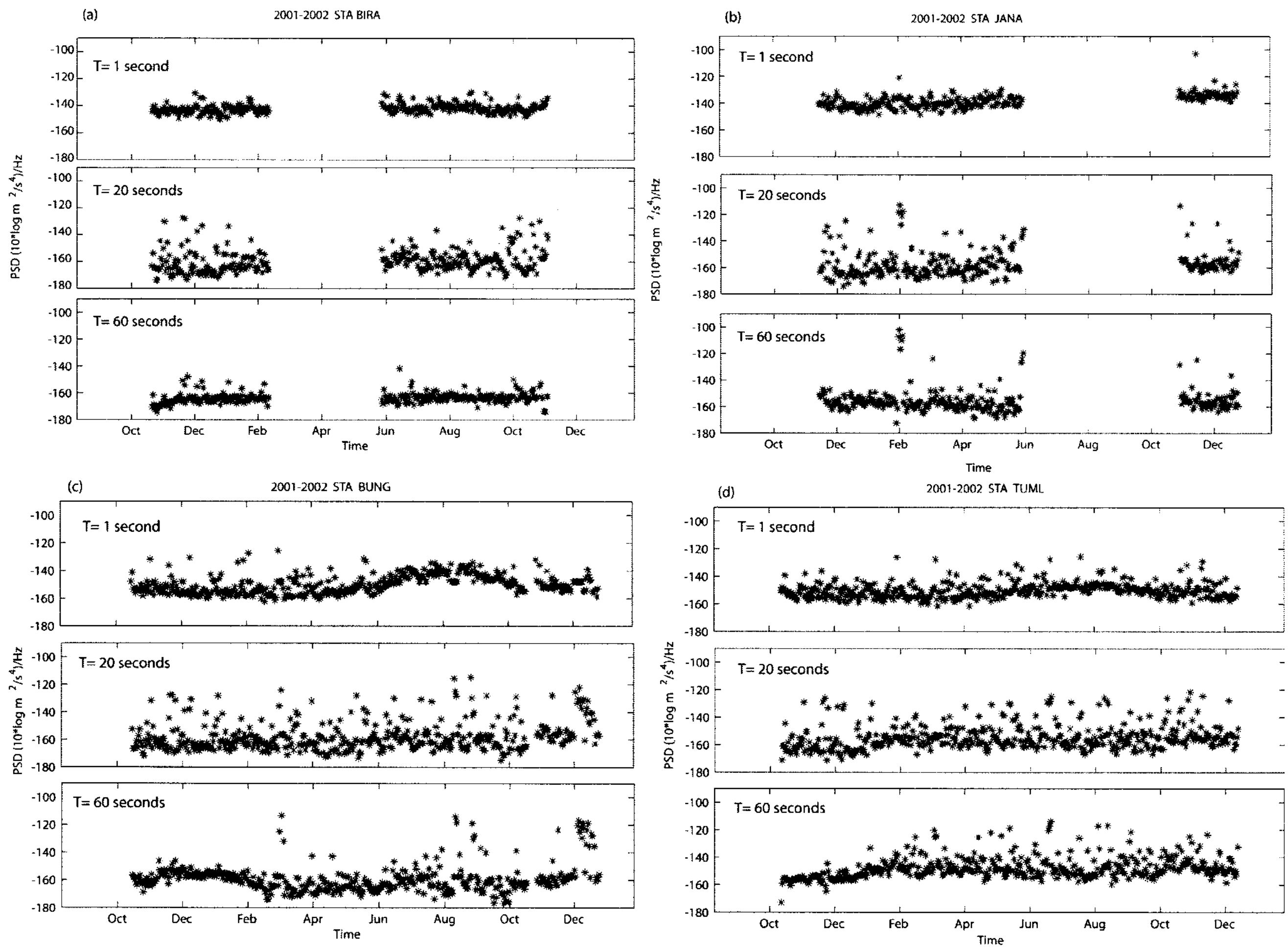

Figure 5. PSD plotted versus time of deployment at periods of 1, 20, and 60 sec for Z component: (a) station BIRA, earthen mound; (b) station JANA, concrete pillar with brick housing; (c) station BUNG, coupled; (d) station TUML, uncoupled.

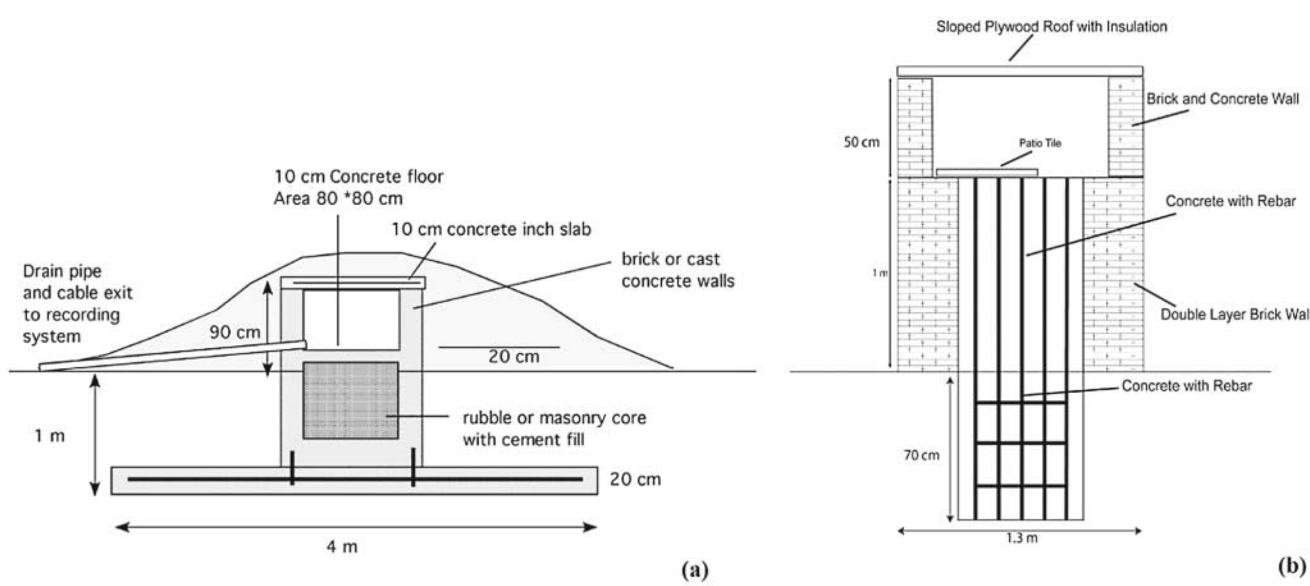

Figure 6. Designs for station BIRA (a) and station JANA (b).

was reflected in the increased variation in the 95% confidence intervals for the Nepal array (Fig. 2).

Conclusion

Compared with the Tibet array the Nepal array was 1–20 dB noisier at frequencies >0.2 Hz, equally noisy in the microseism frequency ranges, and insignificantly quieter at <0.06 Hz for all components. We attribute the greater variation in the short-period >1.0 Hz and long-period <0.06 Hz noise of the Tibet array to the fewer number of days it was in operation than the Nepal array. Day/night variations between the two arrays were similar in the high and microseism frequency bands for all components. However, at long periods, the horizontal components were noisier than the vertical component for the Nepal array, whereas the vertical component was noisier at the most northern Tibet stations. There appears to be a vertical, long-period day time noise source in Tibet, which we do not attribute to wind or tilt because the horizontal components were unaffected.

We expected that sensors placed in different vault types would display contrasts in noise levels as defined by the PSD estimates. This is not the case for the coupled and uncoupled sites even at high frequencies where cultural influences dominate. However, at high frequencies the two stations located in the Ganges River Plain, BIRA and JANA, were noisier than all other stations and displayed no difference whether the sensor was on a concrete pier buried beneath a large earthen mound or set on a pier built above the surface. The mud-mound vault (BIRA) did perform well at long periods, suggesting that neither a cement pad on bedrock nor a cement coupling of the sensor is required to gather data at <0.02 Hz. The uncoupled stations and the coupled stations in Nepal were equally noisy at high frequencies, but coupling seems to have lowered noise by ~5 dB at long periods and reduced the confidence intervals throughout the frequency range. The cement applied around the sensor in the bucket could have stabilized the sensor, diminishing the variability of the noise over time rather than reducing the level. All the stations showed constant noise levels from 1 to 5 days after vault construction and deployment, suggesting that the time cost for acquiring acceptable data is minimal for temporarily deployed stations.

Acknowledgments

We especially thank Dan McNamara for his instructive suggestions early in this study, for providing the algorithm of Peterson (1993), and for comments in review of this article. We thank the Department of Mines and Geology of Nepal and the Chinese Academy of Sciences for assistance with the HIMNT field project. We also thank the PASSCAL Instrument Center at New Mexico Tech for providing the instruments and data-processing assistance. We also thank Harold Bolton for providing the data from station LSA. This material is based on work supported by National Science Foundation Grant 9903066.

References

Peterson, J. (1993). Observations and modeling of seismic background noise, *U.S. Geol. Surv. Open-File Rept. 93-322*, 1–95.

Webb, S. C. (1998). Broadband seismology and noise under the ocean, *Rev. Geophys.* **36,** 105–142.

Welch, P. D. (1967). The use of Fast Fourier Transform for the estimation of power spectra: a method based on time averaging over short, modified periodograms, *IEEE Trans. Audio Electroacoust.* **AU15,** 70–73.

Wilson, D., J. Leon, R. Aster, J. Ni, J. Schlue, S. Grand, S. Semken, S. Baldridge, and W. Gao (2002). Broadband seismic background noise at temporary seismic stations observed on a regional scale in the southwestern United States, *Bull. Seism. Soc. Am.* **92,** 3335–3341.

Department of Geological Sciences and Cooperative Institute
for Research in the Environmental Sciences
University of Colorado at Boulder
Campus Box 399
2200 Colorado Boulevard
Boulder, Colorado 80309
tomd@lithos.colorado.edu
afs@cires.colorodo.edu

Manuscript received 24 May 2004.